

NON-CONSTANT- $\alpha$  FORCE-FREE FIELD OF ACTIVE REGION NOAA 8210S. Régnier<sup>1</sup>, T. Amari<sup>2</sup>, and R. C. Canfield<sup>1</sup><sup>1</sup>Montana State University, Physics Dept, EPS 264, Bozeman, MT 59717, USA<sup>2</sup>Centre de Physique Théorique, École Polytechnique, F-91128 Palaiseau, France

## ABSTRACT

We investigate the 3D coronal magnetic configuration of the active region NOAA 8210 (AR8210). This active region observed on May 1, 1998 is the site of numerous flares. Using the non-constant- $\alpha$  force-free hypothesis, we determine the coronal magnetic field of AR8210. The EIT/SOHO observations and the reconstructed magnetic configuration suggest that the initiation of the eruptive events is related to the existence of a complex topology (e.g. separatrix surfaces). From some characteristic parameters before and after the eruptions, we note that the magnetic energy (the free magnetic budget) decreases by 28% (55%, respectively).

Key words: sun; corona; magnetic fields; flares; non-constant- $\alpha$  force-free field.

## 1. INTRODUCTION

To understand the mechanisms of eruptive events occurring in the solar corona, it is important to determine the 3D coronal magnetic structure of active regions. Assuming a magnetohydrostatic equilibrium, three hypothesis are usually developed (see review by Sakurai 1989): the potential field, the constant- $\alpha$  and non-constant- $\alpha$  force-free field ( $\alpha$  is called the force-free function given by  $\alpha = \frac{J_z}{B_z}$ ). In Régnier, Amari & Kersalé (2002), the non-constant- $\alpha$  force-free (*nlf*) magnetic configuration has been obtained for a simple dipolar active region (classified as a simple topology active region) in which strong electric currents are measured. The authors argue that the triggering of the eruptive event is linked to the presence of a highly twisted flux tube (number of turns greater than 1). In this article, we apply the method developed in Régnier, Amari & Kersalé (2002) to the active region NOAA 8210 (AR8210) which exhibits a complex topology (i.e. existence of separatrix surfaces and no evidence of twisted flux tubes). We also focus our study on the evolution of characteristic parameters *before and after* the eruptive events (Bleybel et al. 1999, 2002) observed in

AR8210: the total magnetic flux through the photospheric surface, the free magnetic energy budget  $\Delta E_m = E_m(nlff) - E_m(pot)$  (difference between the magnetic energy of the *nlf* field and the magnetic energy of the potential field), the relative magnetic helicity  $\Delta H_m$ .

We first describe the active region 8210 (Sect. 2) using both coronal images (EIT/SOHO) and the solar X-ray flux (GOES). In Sect. 3, we highlight the main features of the 3D *nlf* magnetic configuration compared to the coronal observations. We finally summarize the relevant parameters associated with AR8210 before and after the eruptive events (Sect. 4).

## 2. THE ACTIVE REGION NOAA 8210

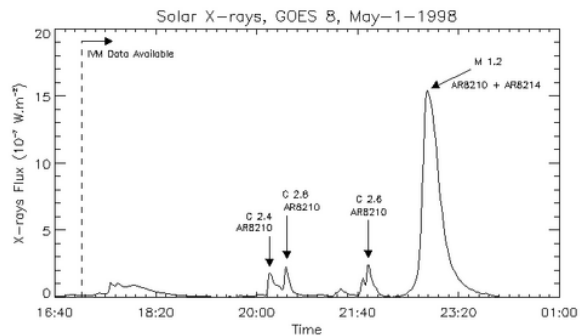


Figure 1. X-rays flux observed by the GOES-8 satellite in the wavelength range 0.5–4 Å. 3 C-class flares and 1 M-class flare are associated with AR8210 between 20:00 UT and 00:00 UT on May 1st. Note that IVM vector magnetograms are available every 3 min during this period.

AR8210 was observed from April 25 to May 9, 1998 in the South hemisphere. During this period, the active region is associated with numerous eruptive events (flares). We here focus on the series of flares observed on May 1st. From 20:00 UT to 00:00 UT, AR8210 produces 3 C-class flares and 1 M-class flare (see Fig. 1). The M-class flare is simultaneously ob-

served in AR8210 and in AR8214 (active region located in the North hemisphere). In Table 1 we summarize the properties of each flare (start time, time when the maximum intensity is detected, end time and class of the flare).

Coronal observations are provided by EIT/SOHO (Delaboudinière et al. 1995). Fig. 2 shows the structure of AR8210 observed in the 195 Å Fe IX/X line. We note that the magnetic topology is well described by this observation: separatrix surfaces appeared clearly on Fig. 2 (see arrows labelled (1), (2) and (3)). We classify AR8210 as a complex topology active region in opposition to simple topology active region studied in a previous work (Régnier, Amari & Kersalé 2002).

*Table 1. Time evolution of the flares related to AR8210 on May 1st from GOES 8 data. Max. Time indicates when the maximum intensity of the flare occurs. (\*) the two consecutive flares are too close in time to define the start time and the end time.*

Start Time	Max. Time	End Time	Class
20:05	20:11	N/A (*)	C 2.4
N/A (*)	20:30	20:35	C 2.8
21:40	21:51	22:01	C 2.6
22:36	22:54	23:08	M 1.2

We study the series of C-class flares observed between 20:05 UT and 20:35 UT (see Table. 1). The magnetic data available for this period are provided by the IVM instrument (Imaging Vector Magnetograph, Mees Solar Observatory, Hawaii; Mickey et al. 1996, Labonte, Mickey & Leka 1999). The spatial resolution is 1.1", the field-of-view is 280" × 280". Using 5 vector magnetograms with a cadence of 3 minutes, we build 15-minutes averaged vector magnetograms with the 180°-ambiguity resolved. This method allows us to reduce the signal-to-noise ratio, especially for the horizontal components of the magnetic field.

### 3. NON-CONSTANT- $\alpha$ MAGNETIC CONFIGURATION

Applying the vector potential Grad-Rubin-like method (Amari et al. 1997, Régnier, Amari & Kersalé 2002), we determine the 3D magnetic configuration of AR8210 before (19:41 UT) and after (21:01 UT) the series of C-class flares. The boundary conditions are given by the vertical component of the magnetic field,  $B_z$  and the distribution of  $\alpha$  on the photosphere. Only  $\alpha$  associated to one chosen polarity is used to transport  $\alpha$  along field lines (see Sakurai 1989). We first verify that the magnetic flux through the photosphere is balanced (see Table 2) since the flux for one polarity is of a few  $10^{22}$  Mx. We also measure the mean value of  $\alpha$ ,  $\alpha_{mean}$ , to estimate the possible connectivity of field lines outside the chosen

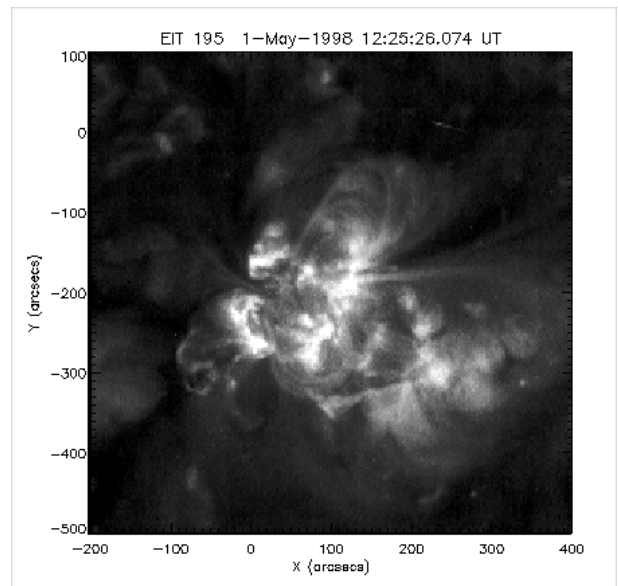


*Figure 2. Fe XII EIT/SOHO image of AR821 on May 1, 1998 at 12:25 UT (field-of-view of 600" × 600", spatial resolution of 2.8"). The arrows (1), (2) and (3) evidence the presence of separatrix surface.*

field-of-view. Knowing that  $\alpha$  values range between -1 and 1  $\text{Mm}^{-1}$ , AR8210 cannot be well described by a potential field reconstruction due to high currents observed on the photosphere.

In Fig. 3, a few characteristic flux tubes are plotted. Comparing Fig. 2 and the magnetic configuration, we confirm that the complex topology observed with EIT can be reduced by the non-constant- $\alpha$  force-free field reconstruction. Note that the same complex behaviour can also be obtained using the potential field method: the separatrix surfaces appeared to be at the same location.

## 4. CONCLUSIONS

Using the method to reconstruct the 3D coronal magnetic field of an active region from photospheric vector magnetograms (Régnier, Amari & Kersalé 2002), the AR8210 magnetic configuration is determined before and after a series of flares.

The magnetic topology for the non-constant- $\alpha$  is close to this for the potential field. We explain this fact by the small values of the electric currents on the photosphere for the field lines close to separatrix. In the case of strong electric currents (Régnier, Amari & Kersalé 2002), we have shown that the magnetic topology and geometry is quite different between the potential and the non-constant- $\alpha$  force-free fields (Régnier 2001). The reconstructed configurations match the coronal observations (195 Å Fe XII EIT image).

Let us recall the definition of the magnetic energy in

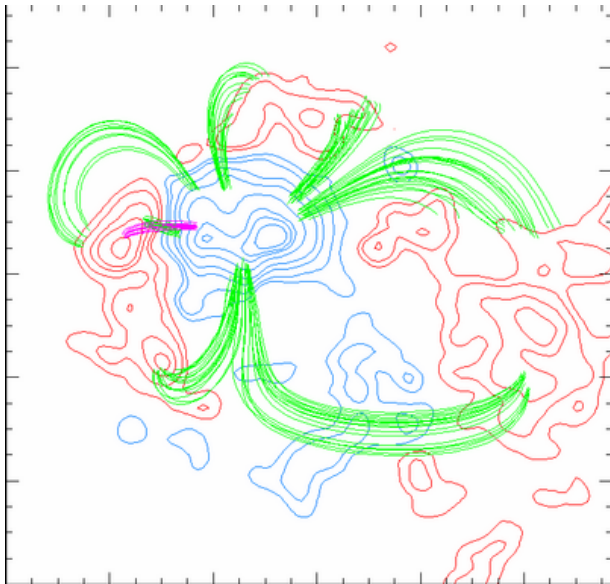


Figure 3. 3D magnetic configuration of AR8210 at 19:41 UT. The plotted flux tubes evidence the existence of separatrix surfaces as observed on Fig. 2. Solid (dashed) contours are positive (resp. negative) magnetic field strength.

the volume  $\Omega$ ,

$$E_m = \int_{\Omega} \frac{B^2}{2\mu_0} dV \quad (1)$$

and the relative magnetic helicity (Berger and Field 1984),

$$\Delta H_m = \int_{\Omega} (\vec{A} - \vec{A}_0) \cdot (\vec{B} + \vec{B}_0) dV \quad (2)$$

where  $\vec{A}$  ( $\vec{A}_0$ ) is the vector potential associated to the *nlff* magnetic field,  $\vec{B}$  (resp. potential field,  $\vec{B}_0$ ).

In order to determine the evolution of AR8210 before and after the eruptive events, we define two kinds of evolving parameters:

- photospheric measurements: from the vector magnetograms measured on the photosphere, we estimate the total magnetic flux through the surface, and the mean value of the force-free function  $\alpha$ ;
- reconstructed parameters: from the 3D non-constant- $\alpha$  force-free reconstruction, we derive the magnetic energy for the potential field,  $E_{pot}$ , and for the *nlff* field,  $E_{nlff}$ , the free magnetic energy budget for the active region and the relative magnetic helicity,  $\Delta H_m$ .

In Table 2, we summarize these parameters for AR8210 observed at 19:41 UT and at 21:01 UT.

Table 2. Time evolution of some relevant magnetic parameters before and after the eruptive event:  $\alpha_{mean}$  mean value of  $\alpha$  on the photosphere,  $E_{pot}$  magnetic energy of the potential field,  $E_{nlff}$  magnetic energy of the non-constant- $\alpha$  force-free field, the free magnetic energy budget is given by  $E_{nlff} - E_{pot}$ ,  $\Delta H_m$  relative magnetic helicity.

	Before	After
$\alpha_{mean} (Mm^{-1})$	$-1.14 \cdot 10^{-2}$	$-7.39 \cdot 10^{-4}$
Magnetic Flux (Mx)	$-5.1 \cdot 10^{20}$	$-14.8 \cdot 10^{20}$
$E_{pot}$ (erg)	$5.08 \cdot 10^{32}$	$3.64 \cdot 10^{32}$
$E_{nlff}$ (erg)	$5.17 \cdot 10^{32}$	$3.68 \cdot 10^{32}$
Free Magnetic Energy Budget (erg)	$9 \cdot 10^{30}$ (1.7%)	$4 \cdot 10^{30}$ (1.1%)
$\Delta H_m (Mx^2)$	$7.48 \cdot 10^{39}$	$1.22 \cdot 10^{40}$

## ACKNOWLEDGMENTS

## REFERENCES

- Amari, T., Aly, J. J., Luciani, J. F., Boulmezaoud, T. Z., Mikic, Z., 1997, *Solar Phys.*, 174, 129
- Berger, M. A., Field, G. B., 1984, *Journal of Fluid Mechanics*, 147, 133
- Bleybel, A., Amari, T., van Driel-Gesztelyi, L., Leka, K. D., 1999, *Proc. 9th European Meeting on Solar Physics*, ESA SP-448, ed. A. Wilson, p. 709
- Bleybel, A., Amari, T., van Driel-Gesztelyi, L., Leka, K. D., 2002, submitted
- Delaboudinière, J. P., et al., 1995, *Sol. Phys.*, 162, 291
- Labonte, B. J., Mickey, D. L., Leka, K. D., 1999, *Sol. Phys.*, 189, 1
- Mickey, D. L., Canfield, R. C., Labonte, B. J., Leka, K. D., Waterson, M. F., Weber, H. M., 1996, *Sol. Phys.*, 168, 229
- Régnier, S., PhD Thesis
- Régnier, S., Amari, T., Kersalé, E., 2002, *A&A*, in press
- Sakurai, T., 1989, *Space Science Reviews*, 51, 11